Quasi-Chemical Viscosity Model for Fully Liquid Slag in the Al_2O_3-CaO-MgO-SiO_2 System. Part II: Evaluation of Slag Viscosities

MASANORI SUZUKI and EVGUENI JAK

A model is presented that enables viscosities to be predicted reliably over the whole range of compositions and temperatures in the Al_2O_3-CaO-MgO-SiO_2 slag system above liquidus in the temperature range from 1543 K to 2643 K (1270 °C to 2370 °C). Experimental procedures and data from the studies reported in the literature have been collected and critically reviewed with particular attention to the viscometry methods and possible contamination of slag samples to select reliable data points for further model development. Relevant revised formalism to describe the complex viscosity trends including charge-compensation effect of the Ca^{2+} and Mg^{2+} cations on the formation of tetrahedrally coordinated Al^{3+} was introduced. Parameters of the quasi-chemical viscosity model have been optimized to reproduce within experimental uncertainties most of the selected experimental data in the Al_2O_3-CaO-MgO-SiO_2 system and all subsystems. This study is part of the overall development of the self-consistent viscosity model of the Al_2O_3-CaO-FeO-Fe_2O_3- MgO-Na_2O-SiO_2 multicomponent slag system.

DOI: 10.1007/s11663-013-9946-1

I. INTRODUCTION

A previous article[1] in this series of two presented the revised formalism of the quasi-chemical viscosity model.[2–7] This work is undertaken as part of the overall development of the self-consistent viscosity model of the Al_2O_3-CaO-FeO-Fe_2O_3-MgO-Na_2O-SiO_2 multicomponent slag system. The current article outlines development of the revised viscosity model[1] for the Al_2O_3-CaO-MgO-SiO_2 slag system, which is a key slag system for a number of metallurgical processes including ironmaking and steelmaking. A number of viscosity measurements has been carried out for this system[8–21] and its subsystems.[22–39] A critical review of experimental procedures and selection of reliable experimental data is an essential stage of the model development. The procedures involved in optimization of the model parameters are reported. The comparisons between the viscosities predicted with the current model and selected reliable experimental data demonstrate agreements within experimental uncertainties over a wide range of temperatures and compositions above liquidus.

The viscosities in this Al_2O_3-containing system have complex trends; in particular, they have the characteristic maximum at the $(Me^{n+})_{2/n}O/Al_2O_3$ ratios around 1. Particular focus in the current article therefore was given to the description and analysis of this characteristic maximum, which is attributed to the so-called "charge-compensation effect" commonly explained by the ability of the Al^{3+} cation to take tetrahedral interstitial between the oxygen anions if the excess negative charge for Al^{3+} is compensated with alkali or alkaline earth cations such as Ca^{2+} and Mg^{2+}, and therefore by the formation of the stronger (Al-O-Metal) covalent bonds. This characteristic maximum was described in the present formalism through the introduction of the probability function expressing proportion of the tetrahedrally coordinated Al^{3+}-containing viscous flow structural units. The Eyring equation[40–42] was used in the current quasi-chemical viscosity model[1–7]; it proved to be adequate to develop a reliable viscosity model to reproduce complex viscous behavior of slag systems. The viscosity equation and parameters for the Al_2O_3-CaO-MgO-SiO_2 slag and its subsystems, and the detail optimization procedures of these parameters, are presented in our previous article[1] of this series of two articles. These model parameters have been optimized using the available experimental viscosity data and some correlations with other physical properties.

MASANORI SUZUKI, formerly Postdoctoral Research Fellow with the PYROSEARCH, School of Chemical Engineering, The University of Queensland, St Lucia, Brisbane, QLD 4072, Australia, is now Assistant Professor with the Division of Materials and Manufacturing Science, Graduate School of Engineering, Osaka University, 2-1 Yamadaoka, Suita, Osaka 565-0871, Japan. Contact e-mail: suzuki@mat.eng.osaka-u.ac.jp EVGUENI JAK, Professor, is with the PYROSEARCH, School of Chemical Engineering, The University of Queensland.

Manuscript submitted April 23, 2013.
Article published online October 1, 2013.

II. REVIEW OF EXPERIMENTAL DATA

Viscosity measurements at high temperatures are difficult to undertake and are subject to a number of composition and temperature uncertainties related to the interaction of slag with crucible and sensor, and to the temperature measurements. A critical and systematic analysis of the experimental procedures therefore is essential to identify reliable experimental data for

Table I. Experimental Conditions of Viscosity Data for the Al_2O_3-CaO-MgO-SiO_2 and its Subsystems

Source	Method, Atmosphere, Temp. Controlling	Container/Sensor Materials	Chemical Analysis after Measurements	Accepted Points
Al_2O_3-CaO			Total:	83
Urbain, 1983[35]	RC; Ar-10 pct H_2; p/m	Mo/Mo	Yes	41
Kozakevitch, 1961[22]	RB; Ar; p/m, t/c	Mo, W/Mo, W	Yes	24
Hofmaier, 1968[24]	RC; Ar; p/m	Mo/Mo	No	18
Al_2O_3-CaO-SiO_2			Total:	911
Kozakevitch, 1961[22]	RB; Ar; p/m, t/c	Mo, W/Mo, W	Yes	213
Toplis, 2004[23]	RB; Air; t/c	Pt-Rh/Pt-Rh	Yes	190
Hofmaier, 1968[24]	RC; Ar; p/m	Mo/Mo	No	38
Machin, 1945 to 1952[16–19]	OB; Air; t/c	Pt/Pt	No	176
Urbain *et al.*, 1982[25]	RC; Ar; p/m	Mo/Mo	Yes	72
Rossin *et al.*, 1964[26]	RC; Ar; p/m	Mo/Mo	Yes	15
Johannsen *et al.*, 1959[13]	RB; N_2; t/c	Pt-Rh/Pt-Rh	Yes	91
Solvang *et al.*, 2004 to 2005[27]	RB; Air; t/c	Pt-Rh/Pt-Rh	Yes	100
Scarfe *et al.*, 1983[20]	RB; Air; t/c	Pt/Pt-Rh	Yes	4
Bills, 1963[29]	RB; N_2; t/c	Ir, Pt/Ir	No	12
Al_2O_3-MgO-SiO_2			Total:	522
Toplis and Dingwell, 2004[23]	RB; Air; t/c	Pt-Rh/Pt-Rh	Yes	99
Hofmaier, 1968[24]	RC; Ar; p/m	Mo/Mo	No	43
Urbain *et al.*, 1982[25]	RC; Ar; p/m	Mo/Mo	Yes	29
Johannsen *et al.*, 1959[13]	RB; N_2; t/c	Pt-Rh/Pt-Rh	Yes	8
Zhilo, 1961[30]	RB; N_2; t/c	Mo/Mo	No	86
Lyutikov and Tsylev, 1963[31]	RB; N_2; t/c	Mo/Mo	Yes	107
Kou *et al.*, 1978[32]	RC; Air; t/c	Pt/Pt	No	40
Machin *et al.*, 1945 to 1952[16–19]	OB; Air; t/c	Pt/Pt	No	28
Riebling, 1964[34]	CBS; Air; t/c	Pt-Rh/Pt-Rh	Yes	90
CaO-MgO-SiO_2			Total:	123
Licko and Danek, 1986[36]	OB; Air; t/c	Pt-Rh/Pt-Rh	No	52
Machin *et al.*, 1945 to 1952[16–19]	OB; Air; t/c	Pt/Pt	No	47
Scarfe *et al.*, 1983[20]	RB; Air; t/c	Pt/Pt-Rh	Yes	6
Urbain *et al.*, 1982[25]	RC; Ar; p/m	Mo/Mo	Yes	7
Yasukouchi *et al.*, 1999[37]	RB; Ar; t/c	Pt-Rh/Pt-Rh	No	11
Al_2O_3-CaO-MgO-SiO_2			Total:	781
Kim *et al.*, 2003[8]	RB; Ar; t/c	Pt-Rh/Pt-Rh	No	8
Kita *et al.*, 2001[9]	OB; Air; t/c	Pt/Pt	Yes	18
Kim et al., 2010[10] and Kim *et al.*, 2013[11]	RB, Ar, t/c	Pt-Rh/Pt-Rh	Yes	83
Liao *et al.*, 2012[12]	RB, Ar, t/c	Mo/Mo	No	0
Johannsen and Brunion, 1959[13]	RB; N_2; t/c	Pt-Rh/Pt-Rh	Yes	13
Forsbacka *et al.*, 2003[14]	RB; Ar-5 pct CO; t/c	Mo/Mo	Yes	79
Song *et al.*, 2011[15]	RB; Ar; t/c	Mo/Mo	Yes	145
Machin *et al.*, 1945 to 1952[16–19]	OB; Air; t/c	Pt/Pt	No	380
Scarfe *et al.*, 1983[20]	RB; Air; t/c	Pt/Pt-Rh	Yes	37
Taniguchi, 1992[21]	CBS; Air; t/c	Pt/Pt	No	18

CBS = counterbalance sphere method; OB = oscillating cup method, p/m = pyrometer; RB = rotating bob method, RC = rotating cup method, t/c = thermocouple.

Table II. Summary of Composition and Temperature Ranges for the Viscosity Measurements in the Al_2O_3-CaO-MgO-SiO_2 System Selected in This Study

Source	Composition Range (Molecular Percentage)				Temperature Range [K (°C)]
	Al_2O_3	CaO	MgO	SiO_2	
Kim *et al.*, 2003[8]	7	42 to 48	7 to 17	34 to 38	1723 to 1773 (1450 to 1500)
Kita *et al.*, 2001[9]	9 to 12	22 to 32	15	45 to 51	1543 to 1775 (1270 to 1502)
Kim *et al.*, 2010[10] Kim *et al.*, 2013[11]	0 to 12	33 to 46	8 to 18	29 to 46	1598 to 1773 (1325 to 1500)
Liao *et al.*, 2012[12]	3 to 10	32 to 35	20	33 - 44	1748 to 1773 (1475 to 1500)
Johannsen *et al.*, 1959[13]	9 to 14	10 to 14	10 to 14	60 to 69	1523 to 1723 (1250 to 1450)
Forsbacka *et al.*, 2003[14]	14 to 19	2 to 10	28 to 53	24 to 41	1853 to 2023 (1580 to 1750)
Song *et al.*, 2011[15]	15 to 19	46 to 63	8 to 16	11 to 23	1720 to 1903 (1447 to 1630)
Machin *et al.*, 1945 to 1952[16–19]	3 to 19	5 to 49	7 to 36	34 to 68	1623 to 1773 (1350 to 1500)
Scarfe *et al.*, 1983[20]	0 to 25	25	0 to 25	50	1548 to 1873 (1275 to 1600)
Taniguchi, 1992[21]	0 to 25	25	0 to 25	50	1573 to 1873 (1300 to 1600)

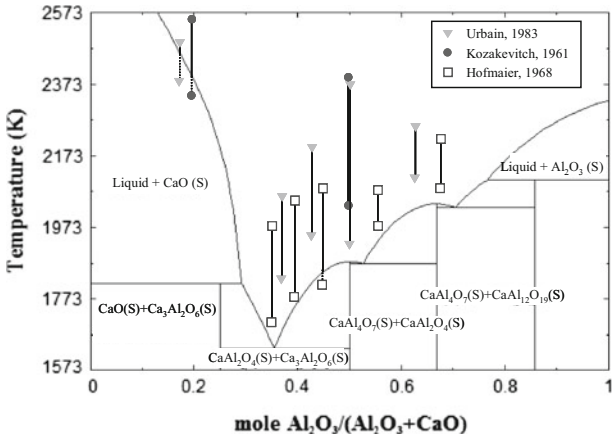

Fig. 1—Compositions and temperature ranges for selected viscosity measurements in the Al_2O_3-CaO system. Liquidus lines are predicted by FactSage.[43]

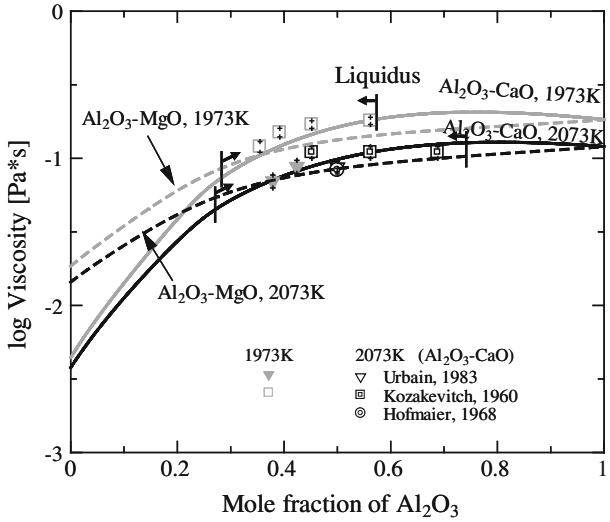

Fig. 2—Calculated viscosities of the Al_2O_3-CaO and Al_2O_3-MgO melt at 1973 K and 2073 K (1700 °C and 1800 °C); Liquidus compositions in the Al_2O_3-CaO system are calculated by FactSage.[43]

further model optimization. All existing experimental viscosity data for the quaternary Al_2O_3-CaO-MgO-SiO_2 system and its subsystems were carefully analyzed in this study with a focus on container and sensor materials, chemical analyses after viscosity measurement, temperature measurements, *etc.*; details of the critical review are given in previous publications.[1–3] Table I summarizes details of the experimental data selected in the current work.

Table II summarizes the temperature and composition ranges of the selected viscosity measurements for the Al_2O_3-CaO-MgO-SiO_2 quaternary system. Kim *et al.*,[8] Kita *et al.*,[9] Kim *et al.*,[10,11] and Liao *et al.*[12] focused on the blast-furnace slag compositions. Because Liao *et al.*[12] reported that some crystalline phases were detected in several slag samples after viscosity measurements and it may affect accuracies of measurements, their results were given low weights in the model optimization. Johannsen *et al.*[13] examined the effect of MgO on the slag viscosity at several compositions in the Al_2O_3-CaO-MgO-SiO_2 system by substituting CaO with MgO at fixed SiO_2 and Al_2O_3 concentrations. Forsbacka *et al.*[14] measured the viscosity of the synthetic slag with relatively low CaO concentrations of interest to the ferrochromium production. Song *et al.*[15] investigated viscosities for the highly basic slag used for secondary refining process in steelmaking. Machin *et al.*[16–19] investigated a wide range of compositions in the Al_2O_3-CaO-MgO-SiO_2 system focusing on the role of alumina and charge-compensation effect on viscosity. Scarfe *et al.*[20] and Taniguchi[21] performed measurements along the diopside ($CaMgSi_2O_6$)–anorthite ($Al_2CaSi_2O_8$) join investigating the relation of magmatic processes to the physical properties of the molten oxides.

III. COMPARISONS OF PREDICTED AND EXPERIMENTAL VISCOSITIES

A. *The Al_2O_3-CaO and Al_2O_3-MgO Systems*

Figure 1 shows the compositions and temperature ranges for the selected data points in the Al_2O_3-CaO system along with the phase diagram calculated using the FactSage computer package (CRCT/GTT Technologies, Montréal, Canada).[43,44] Most of the points were

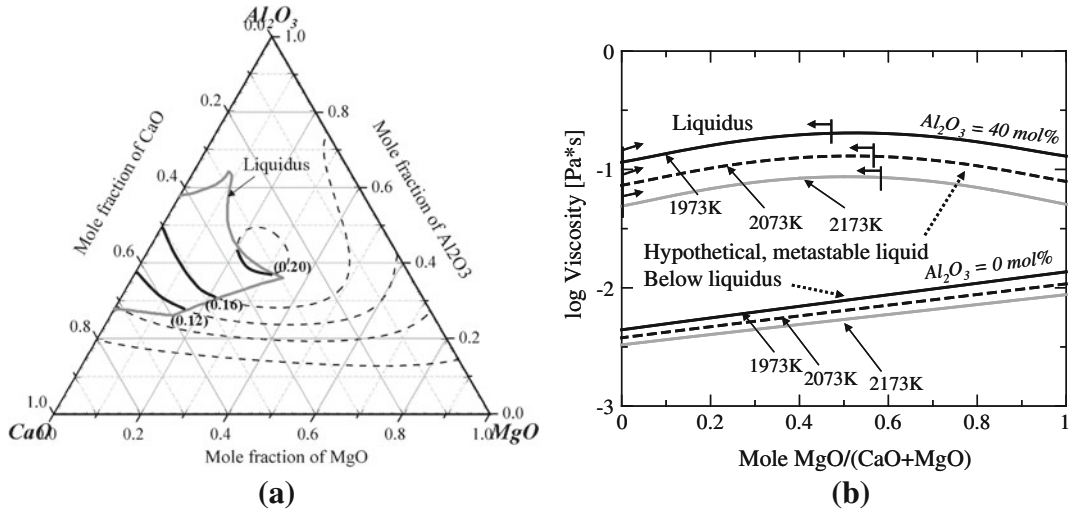

Fig. 3—Calculated viscosity in the CaO-MgO and Al_2O_3-CaO-MgO systems: (*a*) isoviscosity contours at 1973 K (1700 °C) (liquidus line was predicted by FactSage[43]), (*b*) viscosities at 0 or 40 mol pct Al_2O_3 as a function of molar CaO/MgO ratio at 1973 K, 2073 K, and 2173 K (1700 °C, 1800 °C, and 1900 °C).

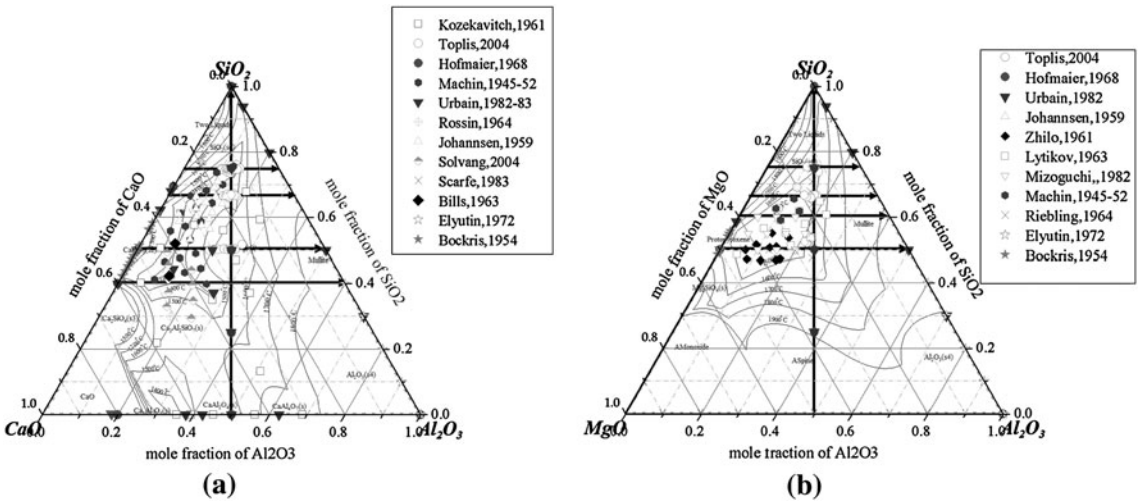

Fig. 4—Compositions of selected viscosity measurements in (*a*) Al_2O_3-CaO-SiO_2 and (*b*) Al_2O_3-MgO-SiO_2 systems along with the liquidus isotherms predicted using FactSage.[43]

measured using the rotating bob or cup method with molybdenum or tungsten as a crucible and sensor materials, and an optical pyrometer for temperature control. As indicated in Table I, Urbain[35] and Kozakevitch[22] measured slag compositions after the viscosity experiments and confirmed that the slag contamination by the dissolution of crucible and sensor materials was negligible. Hofmaier's[24] data were given lower weight because the chemical analysis after experiments was not reported. No experimental data for the Al_2O_3-MgO system were found in the literature.

The predicted viscosities in the Al_2O_3-CaO and Al_2O_3-MgO systems are shown in Figure 2. Note that in Figure 2 and all further figures in this article, viscosities have also been predicted for the liquid compositions below the liquidus temperatures for hypothetical, metastable liquids only for theoretical analysis (this comment refers to all further figures and is not repeated). The viscosity at a fixed temperature changes nonlinearly in those aluminate systems as a function of the Al_2O_3 concentration with distinct maximum at intermediate compositions attributed to the charge-compensation effect and described by the special terms proportional to the proportions of the tetrahedrally coordinated Al^{3+} due to charge compensation by Ca^{2+} or Mg^{2+} cations, respectively. Good agreement between the predicted and experimental viscosities demonstrated in Figure 2 may be taken as an indication of the validity of the introduced formalism.

B. *The Al_2O_3-CaO-MgO System*

The model parameters determined for the Al_2O_3-CaO, Al_2O_3-MgO, and CaO-MgO binary subsystems were used to predict viscosities in the Al_2O_3-CaO-MgO ternary system; Figure 3(a) shows the calculated isoviscosity contours at 1973 K (1700 °C), with the corresponding liquidus line predicted by FactSage.[43]

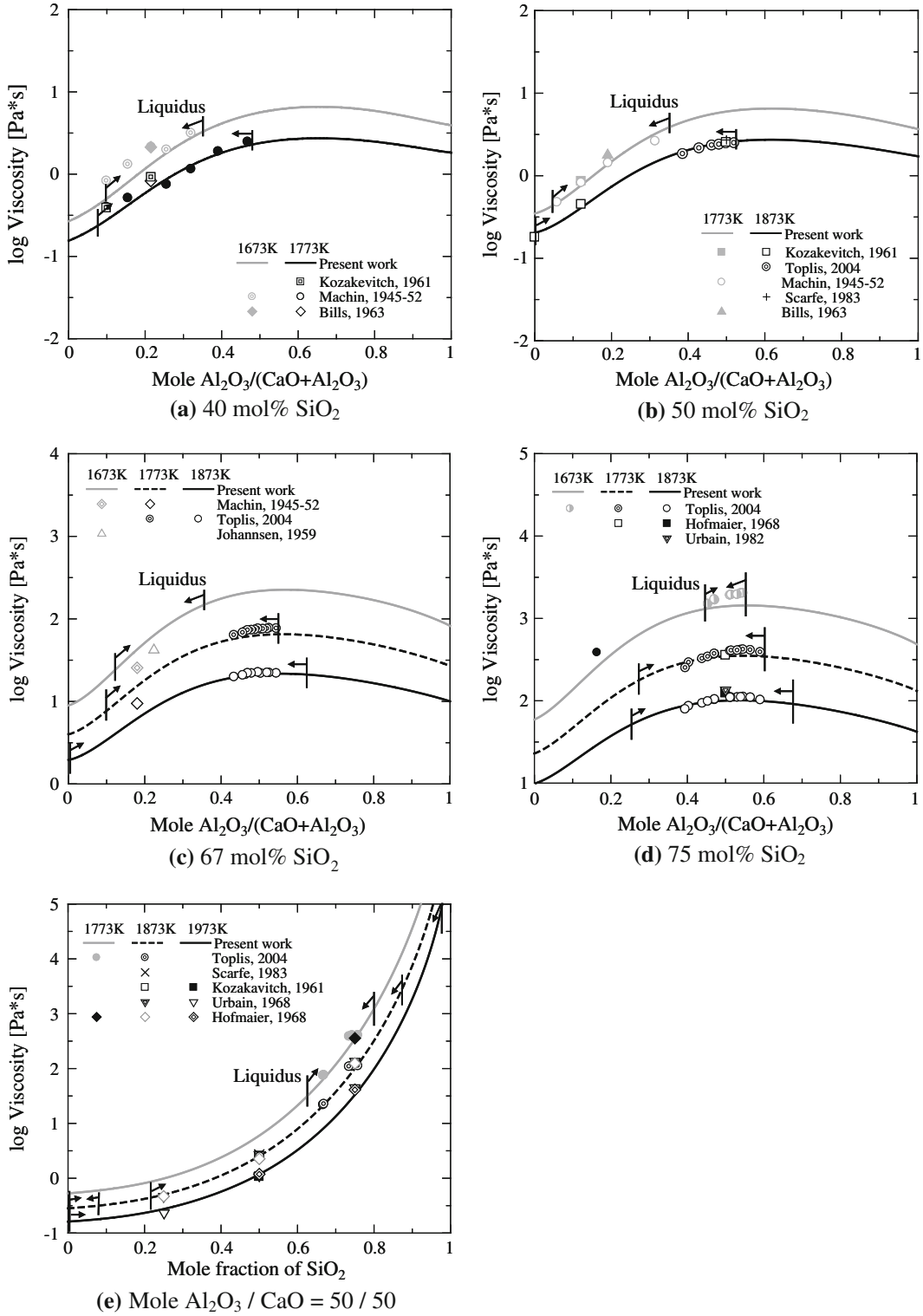

Fig. 5—Comparison of predicted and experimental viscosities in the Al_2O_3-CaO-SiO_2 system: (*a*) 40 mol pct SiO_2, (*b*) 50 mol pct SiO_2, (*c*) 67 mol pct SiO_2, (*d*) 75 mol pct SiO_2, and (*e*) molar ratio Al_2O_3/CaO = 50/50 from 1673 K to 1973 K (1400 °C to 1700 °C). Liquidus is calculated by FactSage.[43]

Although this ternary system is important for refining processes in iron productions, no reliable experimental viscosity data are available. Viscosities as a function of molar ratio MgO/(CaO + MgO) at a fixed Al_2O_3 concentration are shown in Figure 3(b), indicating that the viscosity of the melt is predicted to exhibit maximum at an intermediate compositions in this ternary system (note that predictions at Al_2O_3 = 0 mol pct and in other subliquidus conditions are performed for hypothetical, metastable liquid). This maximum of viscosities

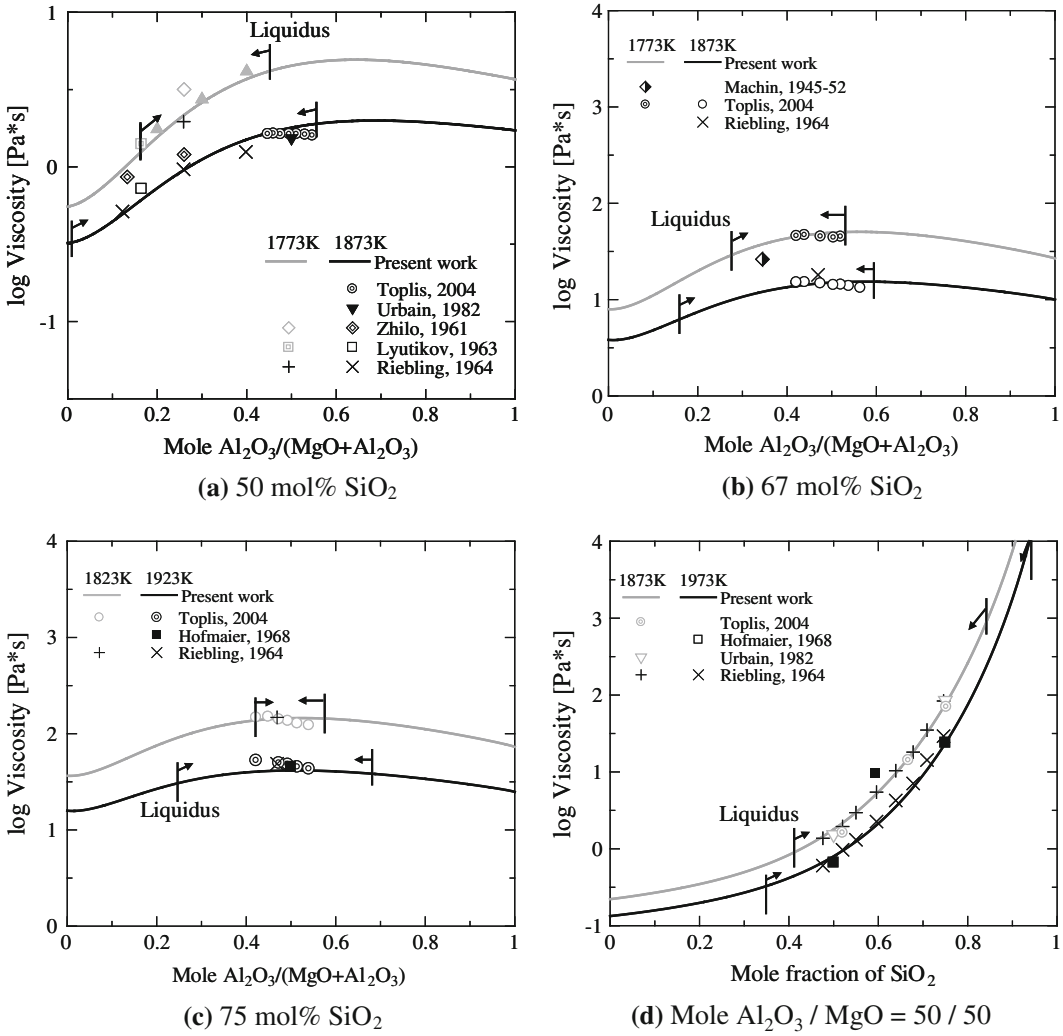

Fig. 6—Comparison of predicted and experimental viscosities in the Al_2O_3-MgO-SiO_2 system along different sections: (*a*) 50 mol pct SiO_2, (*b*) 67 mol pct SiO_2, (*c*) 75 mol pct SiO_2, and (*d*) molar ratio Al_2O_3/MgO = 50/50 from 1773 K to 1973 K (1500 °C to 1700 °C). Liquidus is calculated by FactSage.[43]

at Al_2O_3 mole fraction of ~0.3 and at intermediate MgO/CaO ratios is unexpected; it resulted from the parameters obtained through fitting experimental viscosities for the Al_2O_3-CaO-MgO-SiO_2 quaternary liquids at low SiO_2 concentrations.[14,15]

C. *The Al_2O_3-CaO-SiO_2 and Al_2O_3-MgO-SiO_2 Systems*

The compositions of the selected experimental viscosity data points for the Al_2O_3-CaO-SiO_2 and Al_2O_3-MgO-SiO_2 systems are plotted in Figure 4 along with the liquidus isotherms predicted by FactSage.[43] Slag viscosities have been measured over wide composition and temperature ranges providing a firm basis for the model development. Various sections in ternary diagrams used for a comparison of predictions with experiments given below are illustrated with thick solid lines in Figure 4.

Figures 5 and 6 demonstrate agreement between the model predictions and experimental data in the Al_2O_3-CaO-SiO_2 and Al_2O_3-MgO-SiO_2 systems along different sections with fixed SiO_2 concentrations or fixed Al_2O_3/CaO (or MgO) molar ratios. The predicted viscosities along sections with fixed SiO_2 concentrations have characteristic maximum (upward curvatures) attributed to the "charge-compensation effect" and describe satisfactorily available experimental data.

D. *Analysis of the "Charge-Compensation Effect"*

The "hypothetical" properties $\underline{E}_{a,\text{no charge comp.}}$, $\varepsilon_{V,\text{no charge comp.}}$, $\eta_{\text{no charge comp.}}$, those without assumed contribution of the tetrahedrally coordinated Al^{3+} to the corresponding $\underline{E}_a$ and $\Delta\underline{E}_v$ energies and viscosity, were introduced to analyze the charge-compensation effects by making the probability to form the tetrahedrally coordinated Al^{3+}, $p^{\text{ch,Me}}_{\text{AlO4}}$, equal to zero in the corresponding expressions of the properties $F_{\text{Al}-m} = F^0_{\text{Al}-m} + \sum_{j=\text{Ca,Mg,...}} \Delta F^{\text{ch},j}_{\text{Al}-m} p^{\text{ch},j}_{\text{AlO}_4}$ (where F corresponds to $\overline{E_a}$ or ε_V). The subsequent functions then are

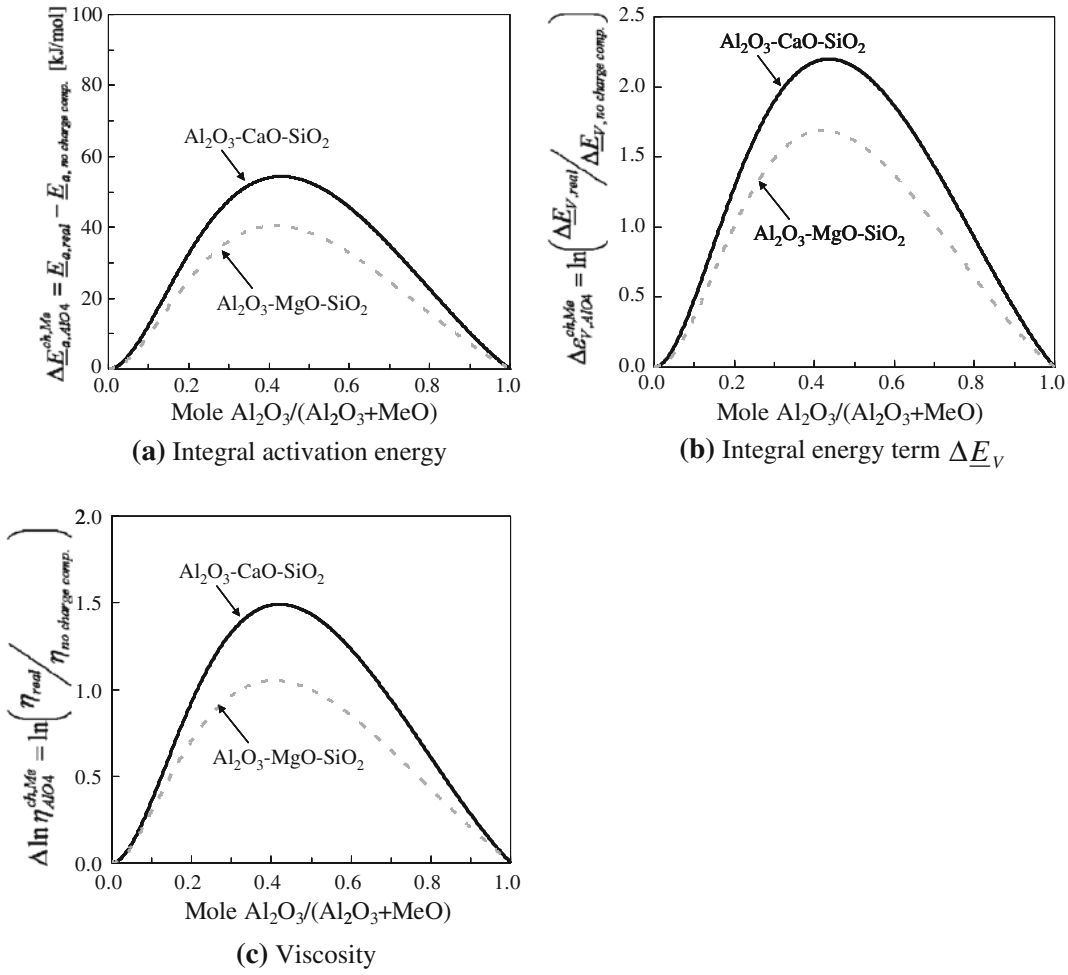

Fig. 7—Predicted charge-compensation effects on (*a*) integral activation energy, (*b*) integral energy term $\Delta \underline{E}_V$ and (*c*) viscosity in Al_2O_3-MeO-SiO_2 melts at 1773 K (1500 °C) where SiO_2 content is kept as 50 mol pct (Me = Ca, Mg).

defined by the following equations expressing the contribution of the charge-compensation effect:

– To the integral activation energy:

$$\Delta \underline{E}^{\text{ch,Me}}_{a,\text{AlO}_4} = \underline{E}_{a,\text{real}} - \underline{E}_{a,\text{no charge comp.}} \quad [1]$$

– to the integral energy term $\Delta \underline{E}_V$:

$$\Delta \varepsilon^{\text{ch,Me}}_{V,\text{AlO}_4} = \ln\left(\Delta \underline{E}_{V,\text{real}} / \Delta \underline{E}_{V,\text{no charge comp.}}\right) = \varepsilon_{V,\text{real}} - \varepsilon_{V,\text{no charge comp.}} \quad [2]$$

– To the viscosity:

$$\Delta \ln \eta^{\text{ch,Me}}_{\text{AlO}_4} = \ln\left(\eta_{\text{real}} / \eta_{\text{no charge comp.}}\right) \quad [3]$$

The charge-compensation effect on the slag viscosity calculated with the Eyring equation[40–42] is the combination of the effects on the $\underline{E}_a$ and $\Delta \underline{E}_v$ energy terms.

Figure 7 shows the predicted charge-compensation effects on the integral activation energy, integral energy term $\Delta \underline{E}_v$, and viscosity in the Al_2O_3-MeO-SiO_2 melts (Me = Ca, Mg) at 50 mol pct SiO_2. The composition dependence of the concentrations of the tetrahedrally coordinated Al^{3+} in the Al_2O_3-CaO-SiO_2 slag was derived from the magnetic-angle spinning nuclear magnetic resonance (MAS-NMR) experimental data[44] and was assumed to be similar in other Al_2O_3-MeO-SiO_2 systems (Me = Mg, Fe^{2+}) due to the lack of experimental information.[1] The charge-compensation effects on the $\underline{E}_a$ and $\Delta \underline{E}_v$ energies and viscosity parameters in those systems were derived from available experimental viscosity data. Figures 7(a) through (c) show satisfactory agreement with experiments and indicate that all those functions are positive over the whole composition range with the maximum close to the Al_2O_3/MeO molar ratio of unity. The charge-compensation effect at a fixed SiO_2 concentration was found to be greater in the Al_2O_3-CaO-SiO_2 system compared to the Al_2O_3-MgO-SiO_2 system in agreement with previous experimental viscosity studies.[23,32]

Figure 8 reports the predicted charge-compensation effects on the integral activation energy, integral energy term $\Delta \underline{E}_v$ and viscosity in the Al_2O_3-MeO-SiO_2 melts (Me = Ca, Mg) as functions of SiO_2 concentration at fixed molar Al_2O_3/MeO ratios of 1.0. Figures 8(a) through (c) indicate that the resulting charge-compensation effect on the $\underline{E}_a$ and $\Delta \underline{E}_v$

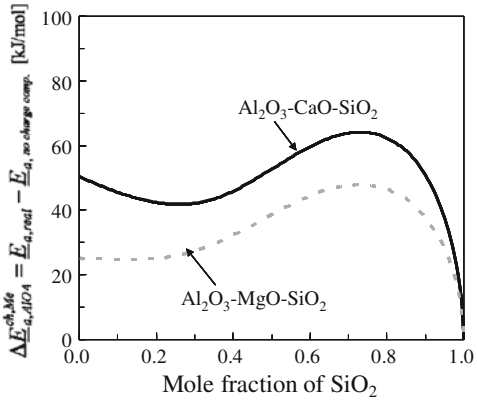

(a) Integral activation energy

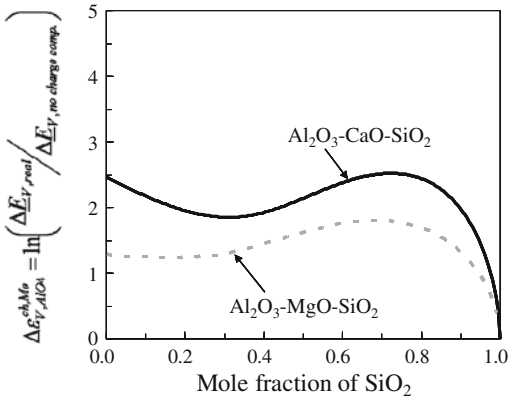

(b) Integral energy term $\Delta \underline{E}_V$

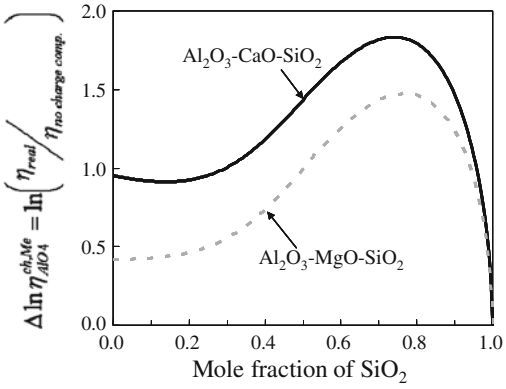

(c) Viscosity

Fig. 8—Predicted charge-compensation effects on (*a*) integral activation energy, (*b*) integral energy term $\Delta \underline{E}_V$, and (*c*) viscosity in Al_2O_3-MeO-SiO_2 melts at 1773 K (1500 °C) where molar ratio Al_2O_3/MeO is kept as 1.0 (Me = Ca, Mg).

energies and viscosity do not change significantly at a low SiO_2 concentrations but increase at high SiO_2 concentrations and exhibit maxima in the range of 60 to 70 mol pct SiO_2. These tendencies at high SiO_2 concentrations are related to the increasing concentrations of the (Al-O-Si) structural units. Note that the Al^{3+} cations taking the tetrahedral rather than octahedral coordination not only form the stronger covalent bonds but also do not weaken the silica tetrahedra covalent bonding, thus having an additional effect of increasing the viscosity.

E. *The Al_2O_3-CaO-MgO-SiO_2 System*

Most of the selected experimental viscosity data[8–21] (see Tables I and II) in the Al_2O_3-CaO-MgO-SiO_2 system were grouped and compositions were projected into pseudoternary sections with approximately 50 mol pct SiO_2 (Figure 9(a)) or with fixed Al_2O_3 concentrations (Figures 9(b) and (c)). The liquidus isotherms calculated using FactSage[43] are also plotted in Figure 9. The viscosity model parameters were optimized to reproduce the experimental data in this quaternary system simultaneously with subsystems; the predicted viscosities in the Al_2O_3-CaO-MgO-SiO_2 system are compared with the corresponding experimental results along the following sections:

(a) 50 mol pct SiO_2, 25 mol pct CaO (diopside – anorthite join), Figure 10(a)
(b) 50 mol pct SiO_2, molar ratio Al_2O_3/MgO = 40/60, Figure 10(b)
(c) 15 mol pct Al_2O_3, 15 mol pct MgO, Figure 10(c)
(d) 19 mol pct Al_2O_3, 8 mol pct MgO, Figure 10(d)

The predicted viscosities reproduce available experimental results as demonstrated in Figures 10(a) through (d). The predicted viscosities increase with increasing Al_2O_3/MgO molar ratio along the diopside–anorthite pseudobinary join (Figure 10(a)) and decrease with the addition of CaO when SiO_2 concentrations are fixed at 50 mol pct and at a constant Al_2O_3/MgO molar ratio of 40/60 (Figure 10 (b)). The latter trend may result from a decreasing charge-compensation effect due to the "excess" of basic oxides (most Al^{3+} took tetrahedral coordination). The predicted viscosities increase as the SiO_2 concentration increases at fixed Al_2O_3 and MgO concentrations (Figures 10(c) and (d)).

Figure 11 shows the predicted viscosities of the Al_2O_3-CaO-MgO-SiO_2 slag as functions of CaO/SiO_2 or Al_2O_3/SiO_2 mass ratios under fixed contents of MgO, compared with some experimental results in the composition ranges used in ironmaking and steelmaking.[10–12,16–19] In Figure 11(a), it was demonstrated that slag viscosities decrease with increasing CaO/SiO_2 mass ratio. The predicted viscosities reproduce well the

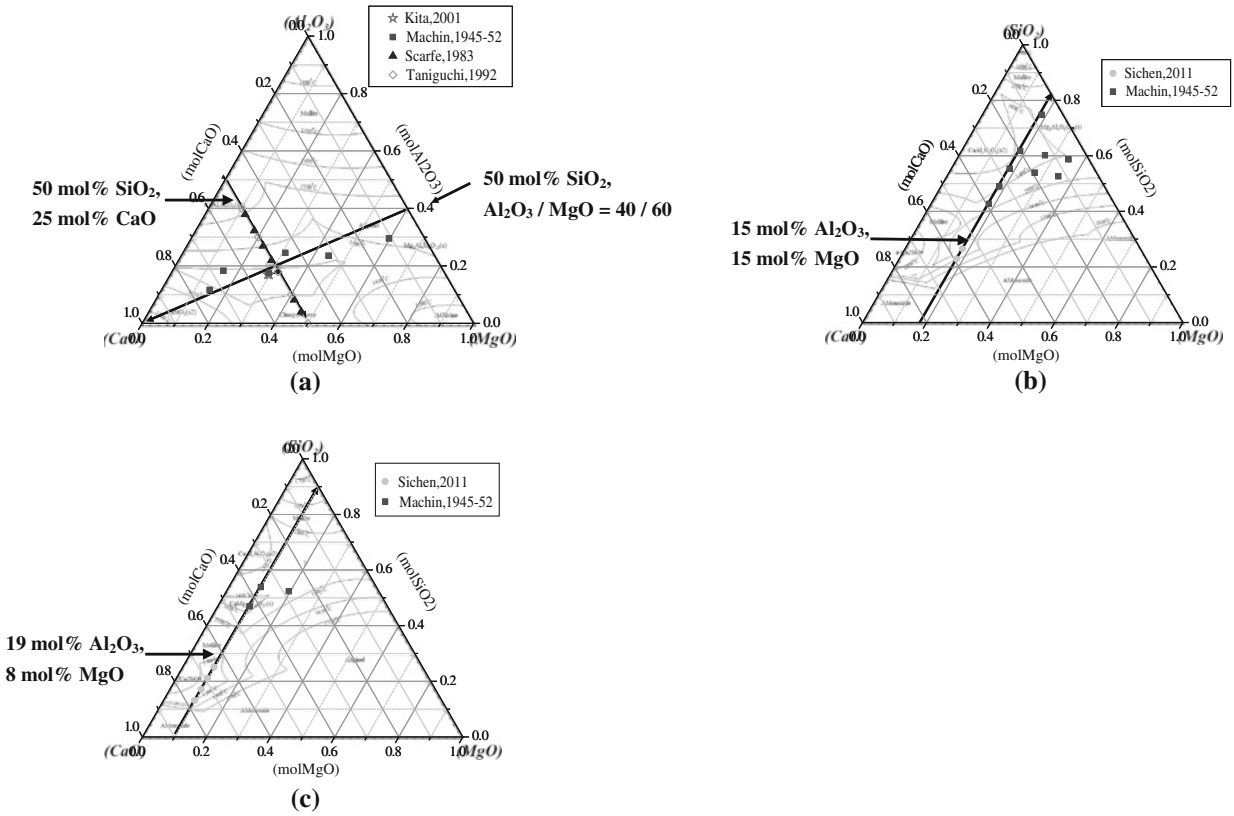

Fig. 9—Compositions of the selected viscosity measurements in the Al_2O_3-CaO-MgO-SiO_2 quaternary system with fixed (*a*) 50 mol pct SiO_2, (*b*) 15 mol pct Al_2O_3, and (*c*) 19 mol pct Al_2O_3 concentrations. Liquidus isotherms are predicted by FactSage.[43]

measured values by Machin *et al.*[16–19] but are lower than values reported by Kim *et al.*[10,11]; the viscosities values reported by Kim *et al.* are higher than those by Machin *et al.* at identical slag compositions. Note that (Si-O-Ca) is the major structural unit in this composition range of the Al_2O_3-CaO-MgO-SiO_2 slag system; the predicted slag viscosities mainly depend on the partial activation energy of the (Si-O-Ca) structural unit determined using the data from the CaO-SiO_2 binary system.

Figure 11(b) demonstrates that the predicted viscosities decrease as the CaO content increases, decrease with the increase of the Al_2O_3/SiO_2 ratio at low CaO concentrations, and remain almost constant or even slightly increase with the increase of the Al_2O_3/SiO_2 ratio at high CaO concentrations; these differences in trends may be attributed to the charge-compensation effect. The predicted viscosities reproduce well the experimental data by Machin *et al.*[16–19]; however, those by Liao *et al.*[12] are high and do not agree with the results by Machin *et al.*[16–19] Liao *et al.* reported that the precipitation of crystalline phase was observed in some slag samples after measurements; therefore, such discrepancies could be caused by the presence of crystalline phases during viscosity measurements.

Figures 12 and 13 present the $\underline{E}_a$ and $\Delta\underline{E}_v$ energies and viscosities, including the charge-compensation effects on the corresponding functions, in the sections of 50 mol pct SiO_2, 15 mol pct Al_2O_3 (Figure 12), 50 mol pct SiO_2, mole CaO: MgO = 1:1 (Figure 13), respectively.

In the constant alumina and silica section (50 mol pct SiO_2, 15 mol pct Al_2O_3, see Figure 12), the charge-compensation effects by Ca^{2+} and Mg^{2+} cations on the $\underline{E}_a$ and $\Delta\underline{E}_v$ energies and viscosities are compared: The effect by Ca^{2+} is stronger than by Mg^{2+} cation for the same concentration of the tetrahedrally coordinated Al^{3+}. The $\underline{E}_a$ and $\Delta\underline{E}_v$ values therefore gradually decrease as the MgO/CaO ratio increases with downward curvatures following the corresponding charge-compensation trends for Ca^{2+} or Mg^{2+}.

In the section with constant 50 mol pct SiO_2 and constant mole CaO:MgO ratio of 1:1 (Figure 13), the$\underline{E}_a$,$\Delta\underline{E}_v$and viscosities have reached maxima at intermediate Al_2O_3 concentrations because little or no Al^{3+} cations are available to be compensated at low $Al_2O_3/(Al_2O_3 + CaO + MgO)$ ratios, and little or no Ca^{2+} and Mg^{2+} cations are available to compensate at high $Al_2O_3/(Al_2O_3 + CaO + MgO)$ ratios.

IV. SUMMARY OF THE COMPARISON OF PREDICTIONS WITH THE EXPERIMENTAL DATA

The calculated viscosities were compared with all selected experimental data for each temperature and

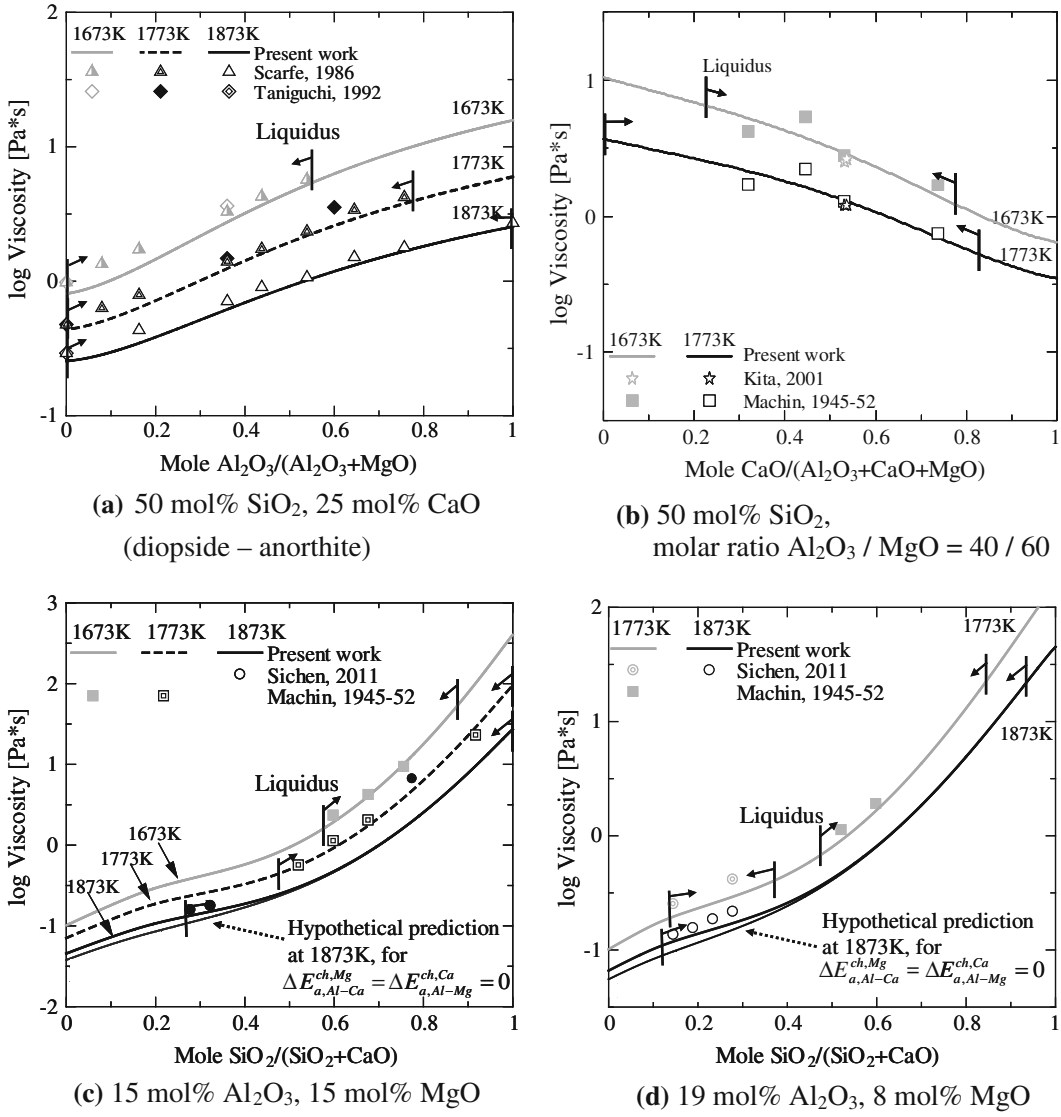

Fig. 10—Predicted slag viscosities of the Al_2O_3-CaO-MgO-SiO_2 system along different sections: (*a*) 50 mol pct SiO_2, 25 mol pct CaO, (*b*) 50 mol pct SiO_2, molar ratio Al_2O_3/MgO = 40/60, (*c*) 15 mol pct Al_2O_3, 15 mol pct MgO, and (*d*) 19 mol pct Al_2O_3, 8 mol pct MgO at 1673–1873 K (1400–1600 °C). Liquidus is calculated by FactSage.[43]

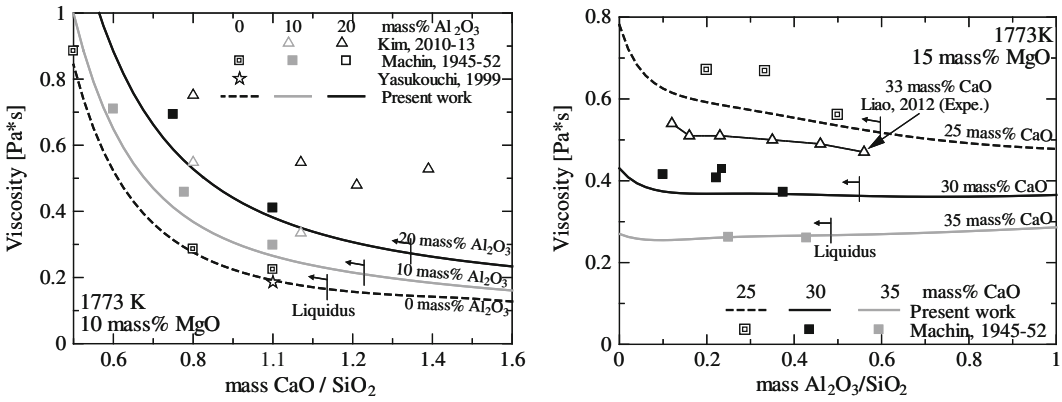

Fig. 11—Predicted viscosities of the Al_2O_3-CaO-MgO-SiO_2 slag at 1773 K (1500 °C); (*a*) as a function of CaO/SiO_2 mass ratio under 10 mass pct MgO and (*b*) as a function of Al_2O_3/SiO_2 mass ratio under 15 mass pct MgO. Liquidus is calculated by FactSage.[43]

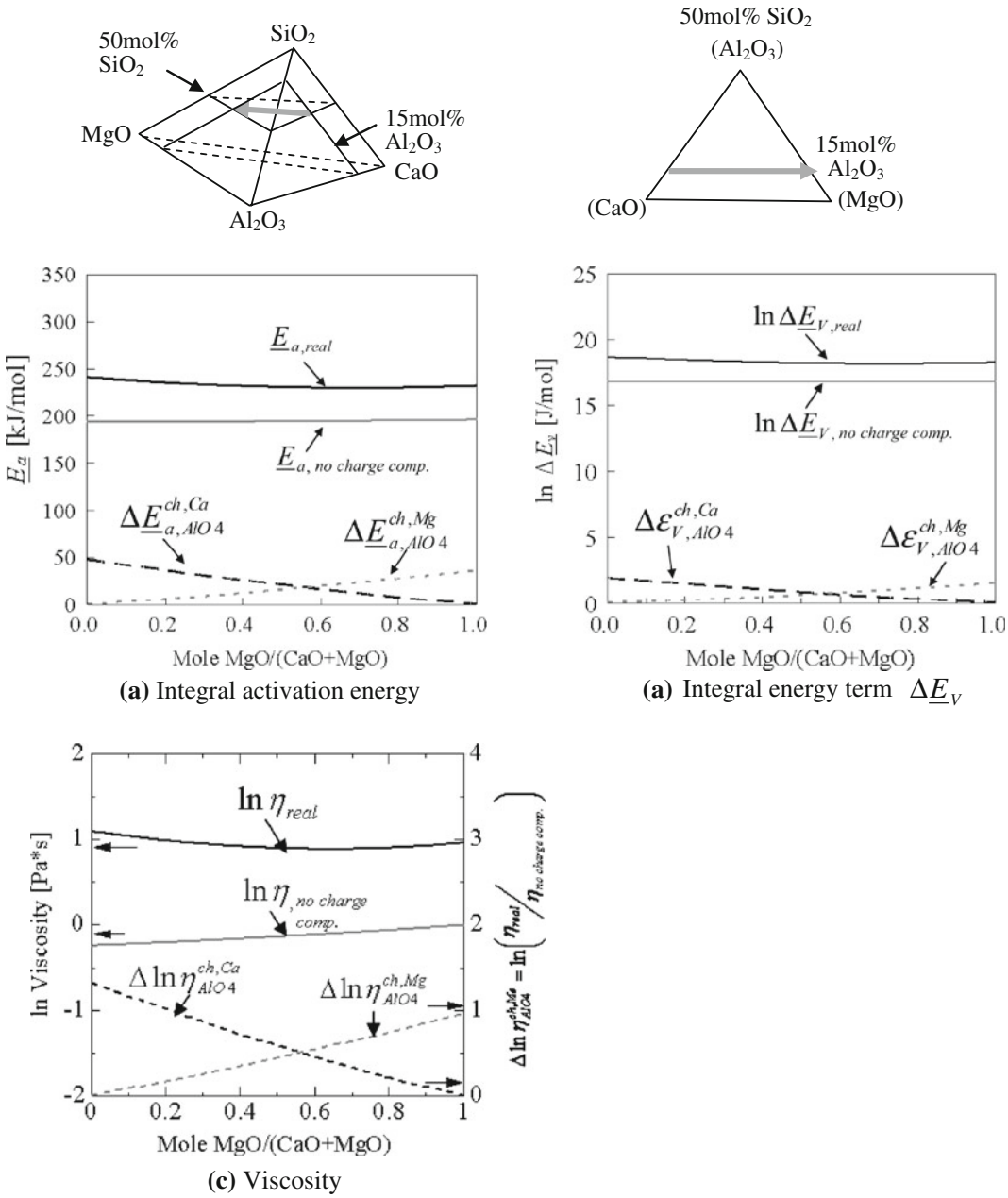

Fig. 12—Calculated results of (*a*) integral activation energy, (*b*) integral energy term $\Delta \underline{E}_V$ and (*c*) viscosity in Al_2O_3-CaO-MgO-SiO_2 melt at 1773 K (1500 °C) (50 mol pct SiO_2, 15 mol pct Al_2O_3).

composition in the Al_2O_3-CaO-MgO-SiO_2 system and its subsystems, as summarized in Figure 14. The Round Robin project[45] previously evaluated the recommended slag viscosity values and the accuracies of viscosity predictions by representative models. In this project, experimental uncertainties of the recommended viscosity measurements were determined as approximately 30 pct. As shown in Figure 14, the current model reproduces almost all available experimental data within experimental uncertainties.

The agreement of the calculated viscosities with experimental values was evaluated by taking the average of relative errors between the calculated and experimental results, described by the following equation:

$$\text{Average of relative errors (pct)} = \frac{100}{N}\sum_{i=1}^{N}\left|\frac{\eta_{\text{Calc},i}-\eta_{\text{Expe},i}}{\eta_{\text{Expe},i}}\right| \quad [4]$$

where N denotes total number of acceptable experimental data points. Figure 15 summarizes the results of analyzing the average of relative errors for the quaternary system Al_2O_3-CaO-MgO-SiO_2 and its subsystems.

The experimental viscosities in the Al_2O_3-CaO-MgO-SiO_2 quaternary system and its subsystems have been accurately reproduced by the revised quasi-chemical viscosity model within experimental uncertainties.

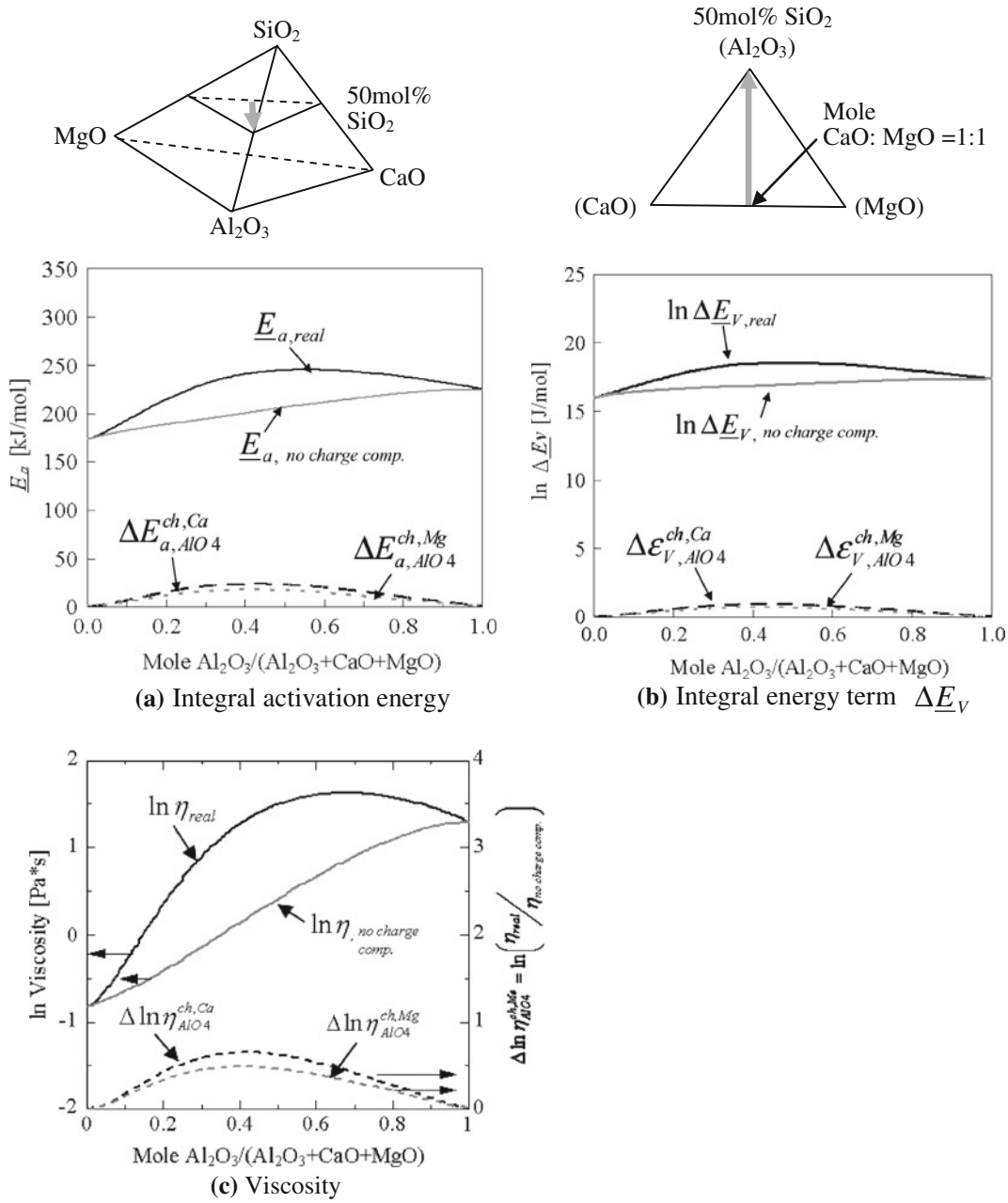

(a) Integral activation energy

(b) Integral energy term $\Delta \underline{E}_V$

(c) Viscosity

Fig. 13—Calculated results of (*a*) integral activation energy, (*b*) integral energy term $\Delta \underline{E}_V$, and (*c*) viscosity in Al_2O_3-CaO-MgO-SiO_2 melt at 1773 K (1500 °C) (50 mol pct SiO_2, mole CaO:MgO = 1:1).

V. EXAMPLES OF MODEL APPLICATION TO ANALYSIS OF VISCOSITIES OF THE INDUSTRIAL SLAGS

Viscosity is one of the key properties important for a number of processes in industrial operations. A careful analysis of the compositional and temperature trends of viscosities is essential for improvements and optimization of the industrial processes. The following example demonstrates how the current viscosity model can be used for the analysis of viscosities in the iron blast furnace slags.

Figure 16(a) shows the predicted isoviscosity contours in the Al_2O_3-CaO-MgO-SiO_2 system with the constant Al_2O_3 concentration of 5 mass pct. This figure demonstrates good agreement of predictions with experimental results reported by Machin *et al.*[16–19] The isoviscosity contours in Figure 16(a) indicate that substitution of MgO with CaO at the constant SiO_2 concentration in slag increases the slag viscosity.

Figure 16(b) shows the viscosity of Al_2O_3-CaO-MgO-SiO_2 iron blast-furnace slag compositions with fixed mass ratios of CaO/SiO_2 = 0.8, 1.0, or 1.2 and constant mass fraction of MgO = 10 mass pct. This figure

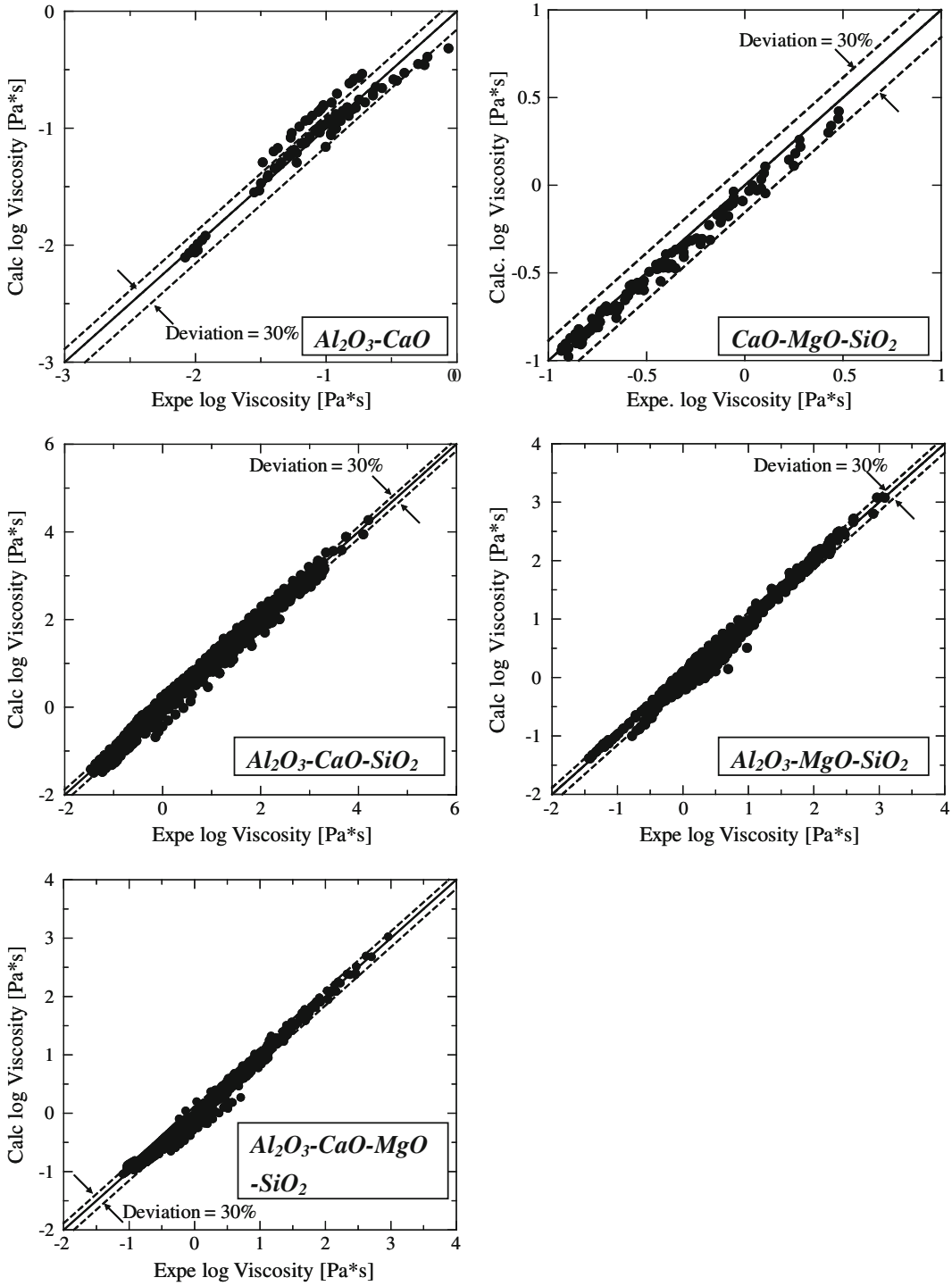

Fig. 14—Comparison between the calculated slag viscosities and all available experimental data in the system Al_2O_3-CaO-MgO-SiO_2 and its subsystems.

demonstrates that viscosity increases with the increase of the Al_2O_3 concentration in the range of iron blast-furnace slags. The increase of the mass ratio of CaO/SiO_2 significantly decreases the slag viscosity; this decrease at lower CaO/SiO_2 ratios between 0.8 and 1.0 is stronger compared to the higher CaO/SiO_2 ratios between 1.0 and 1.2.

VI. CONCLUSIONS

The revised quasi-chemical viscosity model that was developed is capable of predicting the viscosities in the Al_2O_3-CaO-MgO-SiO_2 quaternary system and its subsystems over the wide composition and temperature ranges above liquidus within experimental uncertainties.

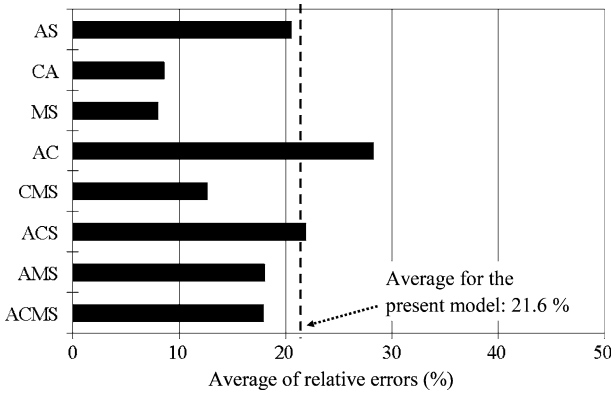

Fig. 15—Average of relative errors between the calculated viscosities and experimental data for the quaternary system Al_2O_3-CaO-MgO-SiO_2 and its subsystems.

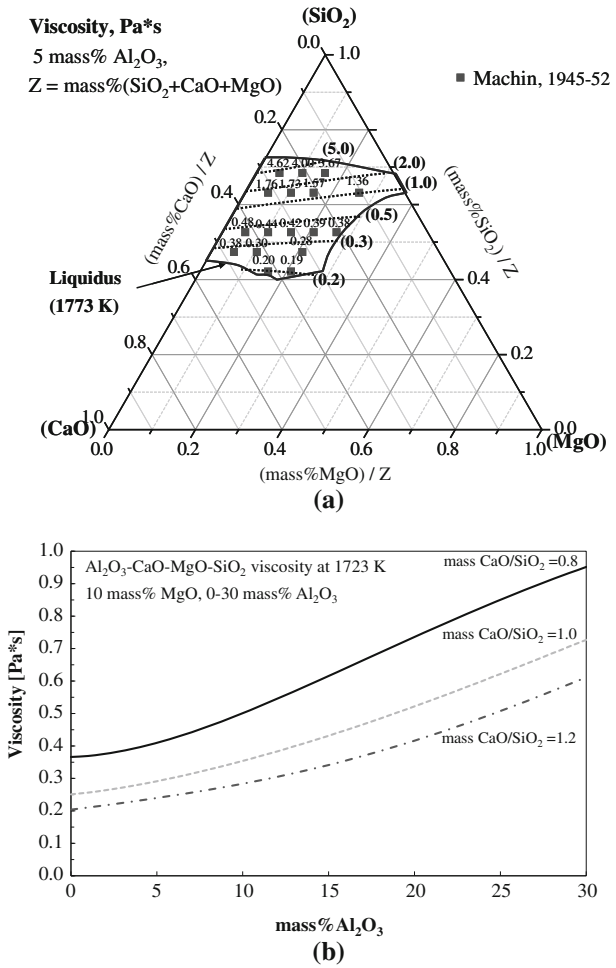

Fig. 16—Predicted (*a*) isoviscosity contours of Al_2O_3-CaO-MgO-SiO_2 slag at 1773 K (1500 °C) where Al_2O_3 mass fraction is kept as 5 mass pct. The liquidus line is calculated by FactSage.[43] (*b*) The viscosity of Al_2O_3-CaO-MgO-SiO_2 slag as a function of Al_2O_3 concentration at 1723 K (1450 °C) under different mass ratios of CaO/SiO_2, where all compositions are included in corresponding liquidus lines obtained by FactSage.

The model describes complex viscosity trends including the so-called charge-compensation effect in this Al_2O_3-containing system. The model can now be used to analyze viscosity trends in the complex industrial slags and thus assist in improvements and optimizations of the current industrial operations and development of new metallurgical processes.

ACKNOWLEDGMENTS

The authors are grateful to Prof. Peter Hayes of the PYROSEARCH, The University of Queensland for useful critical discussions, suggestions on model development, support, and review of the article. The author would like to acknowledge the financial support from the Australian Research Council.

OPEN ACCESS

REFERENCES

1. M. Suzuki and E. Jak: *Metall. Mater. Trans. B*, 2013, in press.
2. A. Kondratiev and E. Jak: *Metall. Mater. Trans. B*, 2005, vol. 36B, pp. 623–38.
3. A. Kondratiev, P.C. Hayes, and E. Jak: *ISIJ Int.*, 2006, vol. 46 (3), pp. 359–67.
4. A. Kondratiev, P.C. Hayes, and E. Jak: *ISIJ Int.*, 2006, vol. 46 (3), pp. 368–74.
5. A. Kondratiev, P.C. Hayes, and E. Jak: *ISIJ Int.*, 2006, vol. 46 (3), pp. 375–84.
6. A. Kondratiev, P.C. Hayes, and E. Jak: *ISIJ Int.*, 2008, vol. 48 (1), pp. 7–16.
7. E. Jak: *Proc. 8th Int. Conf. Molten Slags Fluxes Salts*, Santiago, Chile, 2009, pp. 433–48.
8. J.R. Kim, Y.S. Lee, D.J. Min, and S.H. Jung: *ISSTech 2003 Conf. Prof.*, Indianapolis, IN, 2003, p. 515.
9. Y. Kita, A. Handa, and T. Iida: *J. High Temp. Soc.*, 2001, vol. 27, p. 144.
10. H. Kim, W.H. Kim, I. Sohn, and D.J. Min: *Steel Res. Int.*, 2010, vol. 81, pp. 261–64.
11. H. Kim, H. Matsuura, F. Tsukihashi, W. Wang, D.J. Min, and I. Sohn: *Metall. Mater. Trans., B*, 2013, vol. 44B, pp. 5–12.
12. J. Liao, Y. Zhang, S. Seetharaman, X. Wang, and Z. Zhang: *ISIJ Int.*, 2012, vol. 52, pp. 753–58.
13. F. Johannsen and H. Brunion: *Z. Erzbergbau. Metall.*, 1959, vol. 12, pp. 211–19.
14. L. Forsbacka, L. Holappa, T. Iida, Y. Kita, and Y. Toda: *Scand. J. Metall.*, 2003, vol. 32, pp. 273–80.
15. M. Song, Q. Shu, and D. Sichen: *Steel Res. Int.*, 2011, vol. 82, pp. 260–68.
16. J.S. Machin and D.L. Hanna: *J. Am. Ceram. Soc.*, 1945, vol. 28, pp. 310–16.
17. J.S. Machin and T.B. Yee: *J. Am. Ceram. Soc.*, 1954, vol. 37, pp. 177–86.
18. J.S. Machin, T.B. Yee, and D.L. Hanna: *J. Am. Ceram. Soc.*, 1952, vol. 35, pp. 322–25.
19. J.S. Machin and T.B. Yee: *J. Am. Ceram. Soc.*, 1948, vol. 31, pp. 200–04.
20. C.M. Scarfe, D.J. Cronin, J.T. Wenzel, and D.A. Kauffman: *Am. Mineral.*, 1983, vol. 68, pp. 1083–88.
21. H. Taniguchi: *Contrib. Mineral. Petrol.*, 1992, vol. 109, pp. 295–303.

22. P. Kozakevitch: *Metall. Soc. Conf*., 1961, vol. 7, pp. 97–116.
23. M.J. Toplis and D.B. Dingwell: *Geochim. Cosmochim. Acta*, 2004, vol. 68, pp. 5169–88.
24. G. Hofmaier: *Berg-und Huttenmannische Monatshefte*, 1968, vol. 113, pp. 270–81.
25. G. Urbain, Y. Bottinga, and P. Richet: *Geochim. Cosmochim. Acta*, 1982, vol. 46, pp. 1061–72.
26. R. Rossin, J. Bersan, and G. Urbain: *Rev. Hautes Temp. Refract*., 1964, vol. 1, p. 159.
27. M. Solvang, Y.Z. Yue, S.L. Jensen, and D.B. Dingwell: *J. Non-Cryst. Solids*, 2004, vol. 336, pp. 179–88.
28. M. Solvang, Y.Z. Yue, S.L. Jensen, and D.B. Dingwell: *J. Non-Cryst. Solids*, 2005, vol. 351, pp. 499–507.
29. P.M. Bills: *J. Iron Steel Inst*., 1963, vol. 201, pp. 133–40.
30. N.L. Zhilo: *Izv. Akad. Nauk SSSR, Metall. Toplivo*, 1961, p.17.
31. R.A. Lyutikov and L.M. Tsylev: *Izv. Akad. Nauk SSSR, Metall. Gornoe Delo*., 1963, p. 41.
32. T. Kou, K. Mizoguchi, and Y. Suginohara: *J. Jpn. Inst. Metals*, 1978, vol. 42, pp. 775–81.
33. K. Mizoguchi, K. Okamoto, and Y. Suginohara: *J. Jpn. Inst. Metals*, 1982, vol. 46, pp. 1055–60.
34. E.F. Riebling: *Can. J. Chem*., 1964, vol. 42, pp. 2811–21.
35. G. Urbain: *Rev. Int. Hautes Temper. Refract*., 1983, vol. 20, pp. 135–45.
36. T. Licko and V. Danek: *Phys. Chem. Glasses*, 1986, vol. 27, pp. 22–26.
37. T. Yasukouchi, K. Nakashima, and K. Mori: *Tetsu-to-Hagane*, 1999, vol. 85, pp. 571–77.
38. J. O'M.Bockris and D.C. Lowe: *Royal Soc. London Proc*., 1954, vol. A226, pp. 423–35.
39. V.P. Elyutin, B.C. Mitin, and Y.A. Nagibin: *Fiz. Aerodispersnykh Sist*., 1972, vol. 7, p. 104.
40. H. Eyring: *J. Chem. Phys*., 1936, vol. 4, pp. 283–91.
41. R. Ewell and H. Eyring: *J. Chem. Phys*., 1937, vol. 5, pp. 726–36.
42. S. Glasstone, K.J. Laidler, and H. Eyring: *Theory of the Rate Processes*, McGraw-Hill, New York, NY, 1941.
43. FactSage 6.3, École Poly-technique, Montreal, http://www.factsage.com. Accessed 18 Feb 2013.
44. D.R. Neuville, L. Cormier, and D. Massiot: *Chem. Geology*, 2006, vol. 226, pp. 173–85.
45. K.C. Mills, L. Chapman, A.B. Fox, and S. Sridhar: *Scand. J. Metall*., 2001, vol. 30, pp. 396–403.